

# Photothermal radiometry (PTR) investigation of dynamic thermal parameters of dental composites

M. STREZA\*, D. DADARLAT, M. N. POP, C. PREJMEREAN<sup>a</sup>, D. PRODAN<sup>a</sup>, M. DEPRIESTER<sup>b</sup>, S. LONGUEMART<sup>b</sup>, A. HADJ SAHRAOUT<sup>b</sup>

National R&D Institute for Isotopic and Molecular Technologies, Donath Str. 65-103, POB-700, 400293 Cluj-Napoca, Romania

<sup>a</sup>Raluca Ripan Institute for Research in Chemistry, 400294, Cluj-Napoca, Romania

<sup>b</sup>Univ Lille Nord de France, CP 59000 Lille, ULCO, UDSMM, CP 59140 Dunkerque, France

Thermo-physical properties of some new dental restorative materials were investigated by means of photothermal radiometry (PTR) technique, in order to select the most suitable materials in terms of thermal biocompatibility. The measurement procedure is based on the analysis of the PTR signal (amplitude and phase) as a function of modulation frequency of radiation. The instrumental influence is eliminated by a normalization procedure obtained with a reference sample. The thermophysical parameters were obtained by using some multiparameter optimisation algorithms to fit the PTR experimental data.

(Received November 3, 2010; accepted November 10, 2010)

*Keywords:* PTR radiometry, Dental composites, Thermal diffusivity, Thermal biocompatibility

## 1. Introduction

For several years, photothermal techniques have been successfully applied to the non-destructive investigation of materials-solids, liquids and gases [1-3]. By sending a modulated light onto a sample, the optical energy is absorbed and partially converted into thermal energy. Although the initial absorption processes in many materials are very selective, it is common for the excited electronic states in atoms or molecules to lose their excitation energy by a series of non-radiative transitions that result in a general heating of the material. The resulting periodic heat flux into the sample produces a periodic temperature distribution, which is called *thermal wave*. The analysis of most photothermal effects requires the determination of the temperature field in a medium resulting from conditions, such as a specific type of heating, that may be regarded as imposing specific boundary conditions to the differential equations which govern heat diffusion [4].

In particular, photothermal radiometry (PTR) is one of the most suitable calorimetric techniques because this detection method involves non-destructive, noncontact remote sensing. The technique consists of directing a modulated light beam onto the sample, followed by a change in infrared (IR) Planck spectra of the sample, change which is detected by an IR detector. In a frequency domain experiment, the thermal diffusion length depends on the thermal diffusivity and the modulation frequency. On the other hand, the thermal diffusivity depends, among other things, on micro-structural properties of the material. Thus, an accurate and direct determination of this

parameter gives information about changes that take place as a result either of surface and/or of bulk processes.

Dental composites are complex materials that consist of three major components: organic phase (matrix), inorganic phase (filler) and coupling agent. The resin-based restorative material forms the matrix of the composite material, binding the dispersed glass or silica filler together via the coupling agent [5]. Since the temperature of oral cavity could change dramatically within a few seconds (drinking hot coffee versus eating ice cream), the values of thermal parameters (thermal diffusivity, thermal effusivity and thermal conductivity) should be as close as possible to the enamel and dentin in order to protect the pulp by thermal shock [6]. Concurrently, to minimize the possibility of stress being developed due to the differential expansion and contraction, the coefficient of thermal expansion of a dental composite needs to be as close as possible to that of tooth tissue. Therefore, the knowledge of thermo-physical properties of dental fillers is very important in dentistry [7-9].

## 2. Theory

The layout of the PTR front configuration used in this work is schematically shown in Fig. 1. The first medium air (g) in front of the sample is transparent and semi-infinite, the sample (s) is opaque to the incident visible radiation and in the IR range of detection, and the substrate (b) is also considered semi-infinite. The laser spot size was expanded in order to generate one-dimensional thermal waves. This condition is fulfilled when the laser-beam spot size is at least ten times larger

than the thermal diffusion length in sample at the minimum frequency.

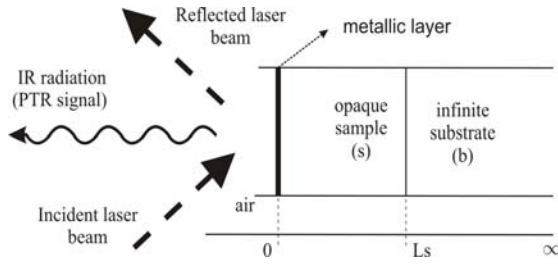


Fig. 1. Layout of the PTR front-detection configuration.

Assuming these experimental conditions, the infrared signal is given by:

$$S(f) = K(f)T_m \quad (1)$$

where  $K$  is an instrumental factor depending on the geometry of the system, the spectral band width of the detector, the emissivity of the surface and on the Stephan-Boltzmann constant, and  $T_m$  is the modulated component of the temperature at sample's surface [4,10]:

$$T_m = \frac{I_0 \eta}{2k_s \sigma_s} \times \frac{1 + R_{sb} \exp(-2\sigma_s L_s)}{1 - R_{sb} \exp(-2\sigma_s L_s)} \quad (2)$$

where  $L_s$  is the thickness of the sample,  $k_s$  is the thermal conductivity of the sample,  $\eta$  is the non-radiative recombination efficiency,  $R$  is the interface thermal wave reflection coefficient,  $I_0$  is optical intensity and  $\sigma_s$  the complex thermal wave number. The complex thermal wave number  $\sigma$  is given by:

$$\sigma = (1 + j)/\mu; \quad \mu = \sqrt{\frac{\alpha}{\pi f}} \quad (3)$$

where  $\mu$  is the thermal diffusion length,  $f$  is the modulation chopping frequency,  $j = \sqrt{-1}$  and  $\alpha$  is the thermal diffusivity. The thermal diffusivity  $\alpha$  is related to the other thermal parameters, the thermal conductivity  $k$ , the thermal effusivity  $e$ , and the mass specific heat  $c$  by:

$$\alpha = \frac{k}{\rho c}; \quad e = \sqrt{\rho c k} \quad (4)$$

with  $\rho$  the density of the material. The interface thermal wave reflection coefficient  $R_{ij}$  between two media ( $i$  and  $j$ ) is given by:

$$R_{ij} = \frac{(b_{ij} - 1)}{(b_{ij} + 1)} \quad b_{ij} = \frac{e_i}{e_j} \quad (5)$$

In order to eliminate the influence of the experimental setup, a normalization procedure of the signal involving the ratio of PTR signals obtained with the substrate and

without substrate was performed. The expression of the normalized signal  $S_n(f)$  is given by:

$$S_n(f) = \frac{S(f)}{S_o(f)} \quad (6)$$

where  $S_o(f)$  is the signal obtained with air as a substrate, and  $S(f)$  is the signal obtained with a well known properties liquid as a substrate. It has been shown [3] that the analytical expression of the normalized PTR signal over the range of experimental interest frequencies has the simplified expression:

$$S_n(f) = \frac{1 + (R_{sb} - 1)\exp(-2\sigma_s L_s)}{1 - (R_{sb} - 1)\exp(-2\sigma_s L_s)} \quad (7)$$

According to Eq.(7), one can obtain the phase  $\theta$  and the amplitude  $S_n$  of the PTR signal respectively [11]:

$$\tan\theta = \frac{-2(R_{sb} - 1)\exp(-2\frac{L_s}{\mu_s})\sin(2\frac{L_s}{\mu_s})}{1 - (R_{sb} - 1)^2 \exp(-4\frac{L_s}{\mu_s})} \quad (8)$$

$$|S_n| = \frac{\sqrt{[1 - (R_{sb} - 1)^2 \exp(-4\frac{L_s}{\mu_s})]^2 + [2(R_{sb} - 1)\exp(-2\frac{L_s}{\mu_s})\sin(\frac{L_s}{\mu_s})]^2}}{[1 - (R_{sb} - 1)\exp(-2\frac{L_s}{\mu_s})\cos(\frac{L_s}{\mu_s})]^2 + [(R_{sb} - 1)\exp(-2\frac{L_s}{\mu_s})\sin(\frac{L_s}{\mu_s})]^2} \quad (9)$$

According to Eqs. (8)-(9), both normalized amplitude and phase of the infrared signal depend on the chopping frequency, on the thermal effusivity of the substrate and on the geometrical and thermal parameters of the sample. Performing a frequency scan of the phase (Eq. 8) one can obtain the smallest value  $f_0$  for which the phase of the PTR signal becomes zero. This leads to the direct determination of the sample's thermal diffusivity:

$$\alpha_s = \frac{4f_0 L_s^2}{\pi} \quad (10)$$

A frequency scan of Eq. (9) leads to the determination of the maximum value of the normalized amplitude which is reached at the frequency:

$$f_1 = \frac{9}{16} f_0 \quad (11)$$

Once known the thermal diffusivity of the sample, its thermal effusivity  $e_s$  can be extracted by using Eqs. (8)-(9). Due to the fact the amplitude of the PTR signal is more sensitive to the intensity fluctuations of the incident radiation and to the surface optical quality of the sample,

the information is usually taken from the phase of the signal.

### 3. Mathematical simulations

If the samples are semi-transparent for the incident radiation, a metallization of the surface exposed to the laser must be done in order to satisfy the theoretical model. Unfortunately, an additional layer can influence the accuracy of the measurement. In order to analyze the influence of additional layers and the diameter of the laser spot on the amplitude and phase of the PTR signals, some mathematical simulations were performed for a “sandwich-type” structure with 4 layers (air/ thin metallic Al layer/  $\text{LiTaO}_3$  crystal/ infinite substrate) [12,13]. The  $\text{LiTaO}_3$  crystal ( $\epsilon=3900 \text{ Ws}^{1/2}/\text{m}^2\text{K}$ ,  $\alpha=1.6 \times 10^{-6} \text{ m}^2/\text{s}$ ) had  $500 \mu\text{m}$  thickness and the substrate was water ( $\epsilon=1600 \text{ Ws}^{1/2}/\text{m}^2\text{K}$ ,  $\alpha=14.6 \times 10^{-8} \text{ m}^2/\text{s}$ ). The results of the simulation are shown in Figs. 2 and 3.

An inspection of Fig. 2 leads to the conclusion that a very thin metallic layer deposited on the sample’s surface doesn’t change the crossing point  $f_0$ , but it affects the shape of the theoretical signal. According to Fig. 3, the one-dimensional heat propagation model is valid down to  $100 \mu\text{m}$  spot laser radius.

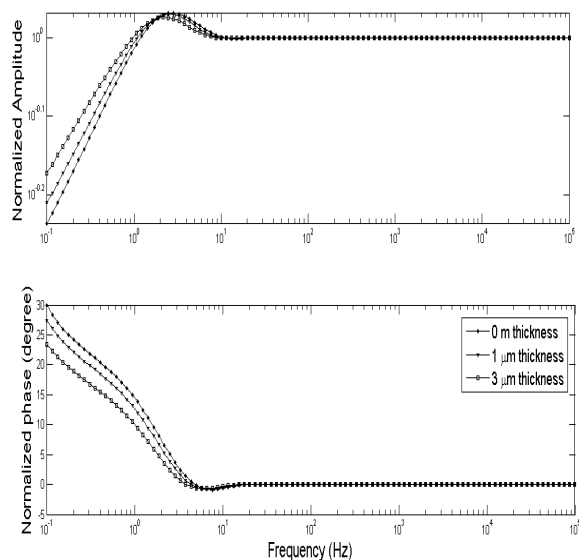


Fig. 2. Theoretical frequency dependence of the normalized PTR signal (amplitude and phase) for different thickness of the metallic (Al) layers. Front medium: air; Sample:  $\text{LiTaO}_3$ ,  $L_s = 500 \mu\text{m}$ ; Substrate: water,  $L_b = 5 \text{ mm}$ .

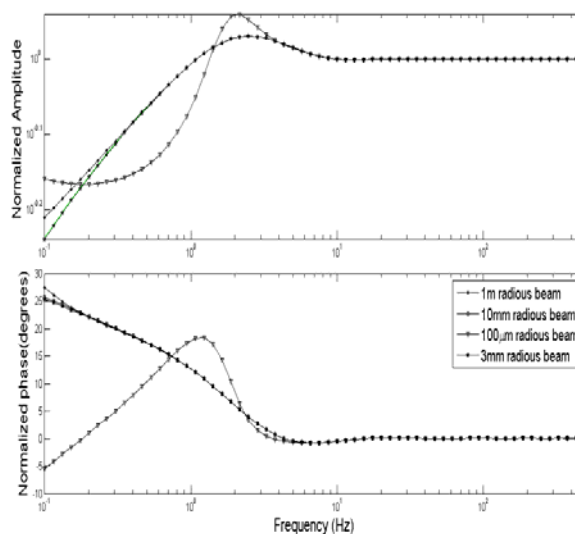


Fig. 3. Theoretical frequency dependence of the normalized PTR signal (amplitude and phase) for different spot laser radius ( $1 \mu\text{m}$  metallic layer). Front medium: air; Sample:  $\text{LiTaO}_3$ ,  $L_s = 500 \mu\text{m}$ ; Substrate: water,  $L_b = 5 \text{ mm}$ .

## 4. Results

### Experimental set-up

The experimental set-up is classical for PTR radiometry, and it was largely presented elsewhere [6-8]. Only few experimental details will be given here. The radiation source is a solid state laser (YAG) with  $\lambda=532 \text{ nm}$  and a controlled power output ( $P=10 \text{ mW}$ ); the radiation is directly modulated from the power laser supply. The size  $D$  ( $5 \text{ mm}$ ) of the laser-beam spot is much larger than the thermal diffusion length in the sample  $\mu$  ( $300 \mu\text{m}$ ) at the minimum chopping frequency ( $1 \text{ Hz}$ ).

The IR radiation from the optically excited sample’s surface was collected and collimated by two off-axis paraboloidal mirrors (Au coated) and focused onto a liquid nitrogen cooled  $\text{HgCdTe}$  (mercury-cadmium-telluride) detector. The heated area of the sample was situated at the focal point of one mirror and the detector was placed at the focal point of the other mirror. The detector had an active area of  $1 \text{ mm}^2$  and a spectral band width of  $1\text{-}12 \mu\text{m}$ . The PTR signal was amplified by a low-noise preamplifier and sent to the digital lock-in amplifier (SR830). The lock-in amplifier received and demodulated the preamplifier output, amplitude and phase of the PTR signal, which were recorded as a function of frequency in a personal computer. The process of data acquisition, storage, and frequency scanning was fully automated.

A series of new copolymers and dental composites have been formulated using two new Bis-GMA-type oligomers ( $\text{P}_2$  and  $\text{P}_3$ ) synthesized at *Raluca Ripan Institute for Research in Chemistry* from Cluj-Napoca. The commercial Bis-GMA (*Merck*) was used as a control.

Triethyleneglicol (TEGDMA) was used as diluting monomer in copolymers and composites. In the composites was used the same filler consisting of a mixture of silanated quarts (50%) and fluorapatite (50%). The composites  $C_2$  and  $C_3$  were prepared as photopolymerizable pastes, by dispersing the filler in the organic resins. The chemical bond between the organic and inorganic phase was provided by silanation of fillers with 3-methacryloyloxypropyl-1-trimethoxysilane (A-174). The powder/liquid ratio was 2,5/1. The results were compared with a composite  $C_1$  synthesized by using the same filler, but a Bis-GMA oligomer ( $P_1$ ) from a commercial company (*Fuji, Japan*). The diameter of the samples was around 7 mm. In order to obtain accurate results, the thickness of the samples, between 200  $\mu\text{m}$  and 300  $\mu\text{m}$ , was strictly controlled. The opacity condition was assured by depositing a thin metallic layer (around 1  $\mu\text{m}$ ) on a side of the sample.

**5. Discussions**

The normalization procedure of amplitude and phase of the PTR signals - with air and water as a substrate- was performed. Analytical procedure in opaque model, involving both amplitude and phase signals for the simultaneous determination of the thermal diffusivity and effusivity of the samples, was used.

To check for the accuracy of the method, a 500  $\mu\text{m}$   $\text{LiTaO}_3$  crystal with well known thermal parameters has been investigated. For this sample, the frequency was scanned from 1 to 20 Hz with a 0.2 Hz step. Fig. 4 presents the normalized phase of the PTR signal compared with the fitting curve (Eq. 8) for a  $\text{LiTaO}_3$  crystal. Fig. 4 indicates a good correlation between experimental data and the best fitting curve.

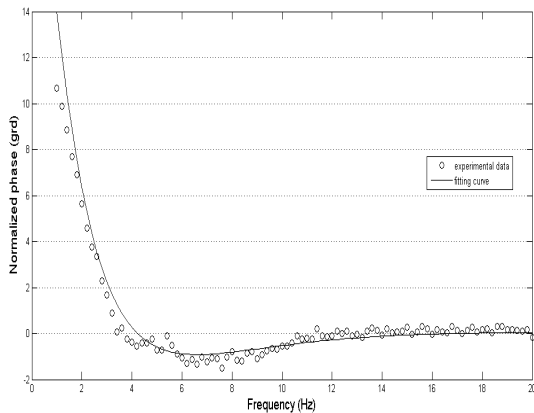


Fig. 4. The fit for the normalized PTR phase obtained with a  $\text{LiTaO}_3$  500  $\mu\text{m}$  opaque sample and with water (5 mm) as semi-infinite substrate.

The phase goes to zero for a frequency  $f_0=4.3$  Hz, which gives for  $\text{LiTaO}_3$  crystal a thermal diffusivity value  $\alpha_s=1.37 \times 10^{-6} \text{m}^2/\text{s}$ . The thermal effusivity value  $e=3930$

$\text{Ws}^{1/2}/\text{m}^2\text{K}$  was obtained from the phase of the signal for different frequencies by using Eq. (8) and taking into account the value of the thermal effusivity of water ( $e=1600 \text{Ws}^{1/2}/\text{m}^2\text{K}$ ). The values of thermal parameters obtained for  $\text{LiTaO}_3$  crystal are consistent with literature data [14, 15].

Figs. 5 and 6 show the typical frequency behaviour of the normalized phase and amplitude of the PTR signal for a 170  $\mu\text{m}$  thick dental composite and water as substrate.

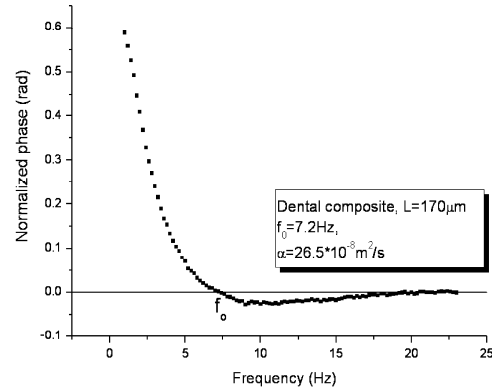


Fig. 5. Normalized phase of the PTR signal obtained with a dental composite sample, and water as substrate.

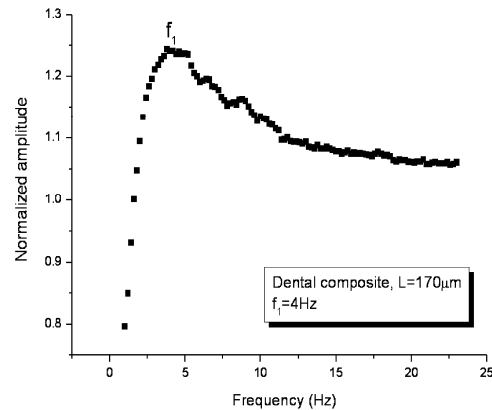


Fig. 6. Normalized amplitude of the PTR signal obtained with a dental composite sample, and water as substrate.

According to Figs. (5) and (6), the maximum amplitude is reached for a frequency  $f_1=4\text{Hz}$ , and the crossing point of the phase for a frequency  $f_0=7.2$  Hz. The experimental values obtained for the particular frequencies  $f_0$  and  $f_1$  are in good agreement with the prediction of Eq. (11) (see Figs. 5 and 6).

In Table 1, the thermal parameters values obtained for samples described above are summarized. The similar experimental and theoretical procedure was used. By using the well-known relationships between thermal parameters, one can obtain the thermal conductivity  $k$ .

Table 1. The dynamical thermal parameters for some new copolymers ( $P_1, P_2, P_3$ ) and dental composites ( $C_1, C_2, C_3$ ).

Sample	$[\alpha \times 10^8] \text{ (m}^2/\text{s)}$	$e(\text{Ws}^{1/2}/\text{m}^2\text{K)}$	$[\text{kx}10^3] \text{ (W/mK)}$
P 1	20.8	1200	5.47
C 1	26.4	830	4.26
P 2	22.3	1600	7.55
C2	26.5	760	3.90
P3	13.2	830	3.01
C3	24.4	1500	7.80

An inspection of Table 1 leads to the conclusion that the thermal effusivity  $e$  and thermal conductivity  $k$  of the investigated samples have not a clear tendency (increasing or decreasing) as a function of composition, while the value of thermal diffusivity depends on the synthesis components. It increases when fillers are incorporated in polymeric matrix, meaning that the inorganic phase changes the thermal properties of the composite (better conducting heat).

## 5. Conclusions

In the paper, the applicability of PTR as a noncontact, non-destructive technique for evaluating the thermal biocompatibility of dental resins has been demonstrated.

A theoretical analysis of the PTR signals leads to the conclusion that a very thin metallic layer deposited on the sample's surface doesn't change the crossing point  $f_0$ , but it affects the shape of the theoretical signal. Due to this fact, the accuracy obtained for the thermal effusivity is lower than in case of thermal diffusivity.

The normalized PTR signal allows the direct, simultaneous measurement of thermal diffusivity and effusivity of a solid sample at a given temperature; no calibration procedure is requested. Although the thermal diffusivity could be obtained by using both amplitude and phase, a better accuracy and reproducibility was obtained when the information was taken from the phase.

Concerning the investigated samples, a good correlation between experimental and theoretical data for a  $\text{LiTaO}_3$  crystal was obtained [14, 15]. The values found for the thermal parameters of new synthesized dental resins are close to those of dentin and enamel [6], indicating that all investigated materials can be safely used without causing any pulpal response.

Due to the fact that the PTR signal carries out information about heat transport rate through the sample, work is in progress with the study of the polymerization depth profile of polymerized dental resins.

## Acknowledgements

Authors thankfully acknowledge for providing research facilities Romanian Ministry of Education and

French Ministry of Foreign Affairs, which supported the Bilateral Brancusi Research Project (NIRDIMT Cluj-Napoca - Univ. Littoral Dunkerque).

## References

- [1] H. Vargas, L. C. M. Miranda, Phys. Rep. **43**, 161, (1988).
- [2] D. Almond, P. Patel, Photothermal Science and techniques, Chapman and Hall Press, London, (1996).
- [3] D. Dietzel, A. Hadj-Daoud, K. Simon, B. K. Bein, J. Pelzl, Anal. Sci. **17**, s189 (2001).
- [4] A. Mandelis, Diffusion Wave Fields, pp. 124-130, Springer, Berlin (2001).
- [5] R. D. Jackson, M. Morgan, J. Am. Dent. Assoc. **131**, 375 (2000).
- [6] M. Lin, F. Xu, T. J. Lu, B. F. Bai, Dental Materials **26**, 501, (2010).
- [7] L. Nicolaides, A. Mandelis, C. J. Beingsner, J. Appl. Phys. **89**, 7879 (2001).
- [8] Y. Liu, N. Baddour, A. Mandelis, C. J. Beingsner, J. Appl. Phys **96**, 1521 (2004).
- [9] P. Martinez-Torres, A. Mandelis, J. J. Alvarado-Gil, J. Appl. Phys. **106**, 114906 (2009).
- [10] B. K. Bein, J. Bolte, D. Diesel, A. Hadj Daoud, G. Kalus, F. Macedo, A. Linnenbrgger, H. Bosse, J. Peltzl, Surf. Coat. Technol **116-119**, 147 (1999).
- [11] M. Depriester, P. Hus, S. Delenclos, A. Hadj Sahraoui, Rev. Sci. Instrum. **76**, 074902 (2005).
- [12] C. Glorieux, J. Fivez, J. Tohen, J. Appl. Phys **73**, 684 (1993).
- [13] G. Kalogiannakis, D. Van Hemelrijck, S. Longuemart, J. Ravi, A. Okasha, C. Glorieux, J. Appl. Phys **100**, 063521 (2006).
- [14] A. H. Sahraoui, S. Longuemart, D. Dadarlat, S. Delenclos, C. Kolinsky, J. M. Buisine, Rev. Sci. Instrum. **73**, 7 (2002).
- [15] M. Nakamura, S. Takekawa, K. Kitamura, Opt. Mat. **32**, 1401 (2010).

---

\*Corresponding author: [streza.mihaela@gmail.com](mailto:streza.mihaela@gmail.com)